Structure *15*

Supplemental Data

Structure and Analysis of FCHo2 F-BAR Domain:

A Dimerizing and Membrane Recruitment Module

that Effects Membrane Curvature

William Mike Henne, Helen M. Kent, Marijn G.J. Ford, Balachandra G. Hegde, Oliver Daumke, P. Jonathan G. Butler, Rohit Mittal, Ralf Langen, Philip R. Evans, and Harvey T. McMahon

Including:

Crystal Structure Determination & Refinement

Isomorphous replacement phasing. The two EMTS derivative crystals each had three major mercury binding sites, located on Cys86: the other two cysteines, residues 47 & 273, were not available because they formed a disulphide bond in the crystal. These sites were located easily by SHELXD: the difference Patterson is very clear (figure S1). The isomorphous differences provided excellent phases at low resolution, but tailing off quite rapidly with increasing resolution. Solvent flattening (61% solvent content) produced a very clear electron density map (Figures S2, S3).

Figure S1

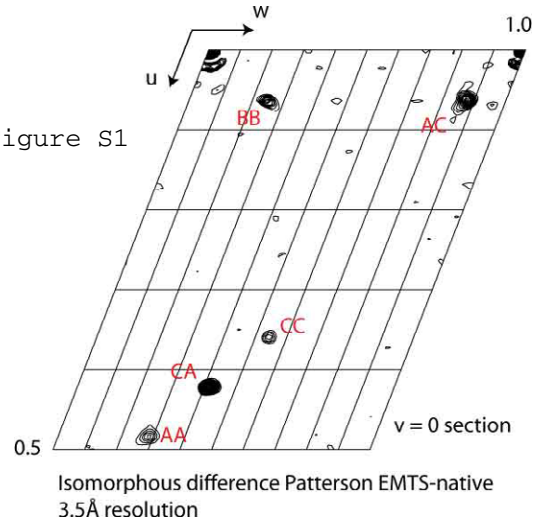

Isomorphous difference Patterson EMTS-native
3.5Å resolution

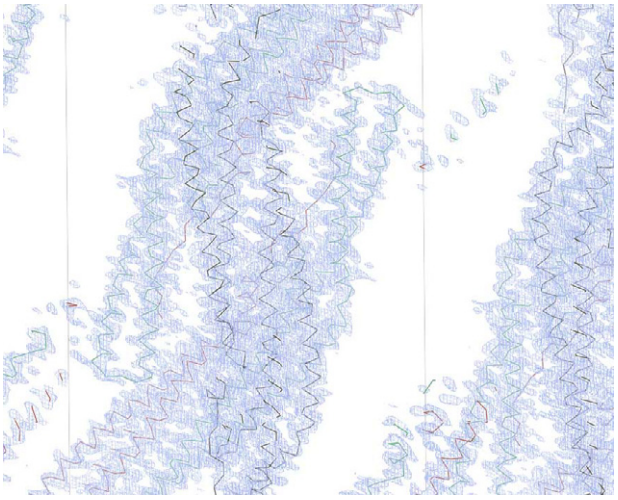

(a)

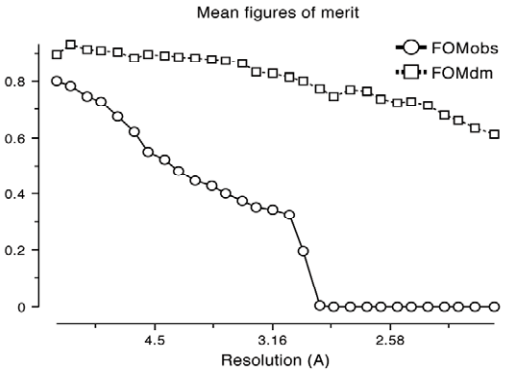

Figure S2. Phasing Statistics from Sharp & Solomon

Figure S3. Solvent-Flattened Experimental Phased Electron Density Map, with Final Refined Model Superimposed. (a) Overview, showing the long helices

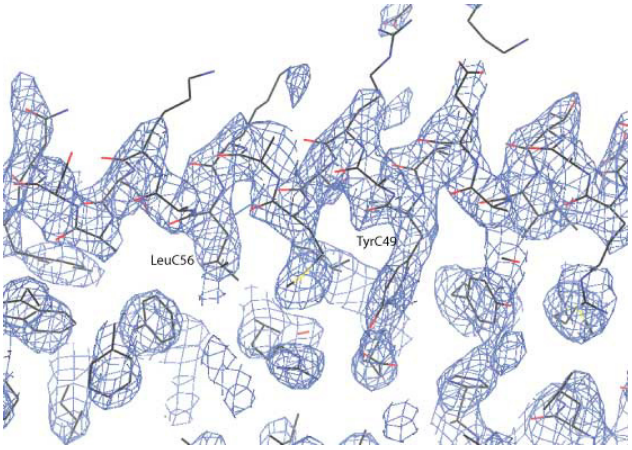

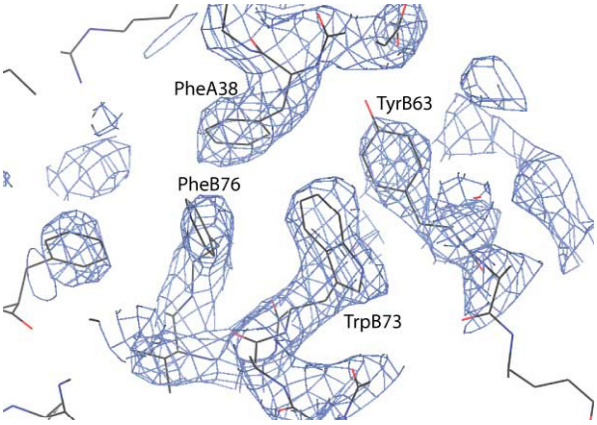

Refinement. The model was refined with REFMAC5, initially using main-chain hydrogen bond restraints in the helical regions (with breaks at the kinks) to keep the helical stereochemistry regular. Non-crystallographic symmetry restraints between the three monomer chains were tried at various stages in the refinement process, but made little difference to the maps or the R-factors: the three subunits were very similar (figure S4). The R-factors from the refinement are rather higher than would be expected for a 2.3Å resolution structure: this can probably be attributed to the marked anisotropy in the data (range of principal components of anisotropic B-factors is 37Å^2). Despite this, the maps were clear and there was no problem in the initial model building, the correction of errors, nor in the placing of water molecules, and the correlation between observed and calculated electron density is good throughout all of the structure except the end of some loops.

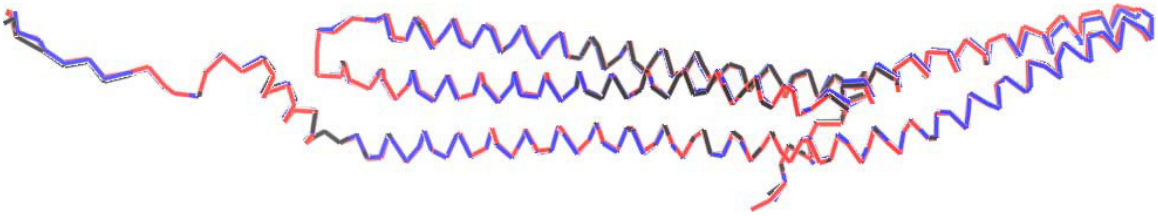

Figure S4. Ca Atoms of the Three Subunits Superimposed (Red, Blue, Black)

The structure is very largely helical (figure S5), apart from the extreme C-terminus, which also contains a disulphide link between residues Cys147 and Cys273 in different subunits of each dimer (figure S6): this bond would presumably not exist in the reducing environment of the cytoplasm.

QuickTime™ and a
TIFF (LZW) decompressor
are needed to see this picture.

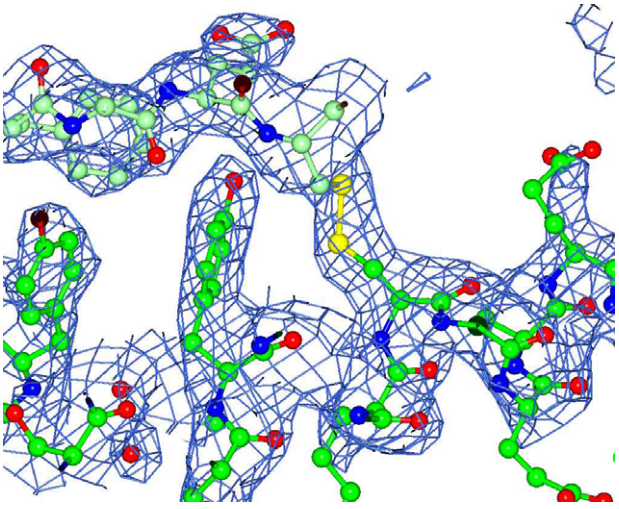

Figure S6. Electron Density ($2mF_o$-DF_c) around the CysA147-CysB273 Disulphide Bond

Figure S5. Ramachandran Plot

Ultracentrifugation

The weight average molecular mass $\left(\bar{M}_{w,app}\right)$ was determined by sedimentation equilibrium, using a Beckman XL-A analytical ultracentrifuge. Samples at different loading concentrations were sedimented at 10,000 rpm at 20.0 ºC in double sector cells with 12 mm pathlength, in an An 60 Ti rotor. Initial overspeeding (at 150% of the final equilibrium speed) was carried out for 6 h, to reduce the time to reach equilibrium [1]. After the overspeeding, interference scans were taken at 24 h intervals, and, when successive scans were indistinguishable, the sedimentation was taken to be operationally at equilibrium.

Initially, data were analysed for each cell by taking overlapping sets of 101 datum points, taken to be at the concentration of the middle point, and weight average molecular masses calculated by non-linear regression, using equation [2]:

$$\bar{M}_{w,app} = \frac{d\ln c_2}{dr^2}\frac{2RT}{(1-\bar{v}\rho)\omega^2} \;;$$

where c_r is the protein concentration at radius r, R and T are the gas constant and temperature (in degrees K), ω is the angular velocity (in rad/sec), $\bar{v}$ the partial specific volume and ρ the solvent density, both of these latter were calculated using the program SEDNTERP [3]. Regression analysis and subsequent plotting of the results was made with the programme ProFit, version 5.6.7 (Quantum Soft, Zürich, Switzerland).

Inspection of the plots of $\bar{M}_{w,app}$ against c_r suggested that the protein was behaving as a monomer/dimer equilibrium and this was investigated further by directly fitting the data for c_r against r, giving a closer approximation to random Gaussian error and therefore a better analysis by least-squares to estimate the parameters [4] (again using ProFit, using the Levenberg-Marquardt algorithm). The equation used can be simplified by taking:

$$\sigma = \frac{M_1(1-\bar{v}\rho)}{2RT} \;;$$

when the protein concentration c_r at radius r becomes:

$$c_r = \left(\rho c_0 (r-r_0)^2 + 2\left(\frac{\left(\rho c_0 (r-r_0)^2\right)^2}{K_d} \right) \right);$$

where c_0 is the concentration (expressed as monomer) at reference radius r_0, K_d is the dissociation constant.

Plots of the residuals between the measured and calculated optical density were made to check the validity of the model used, and also plots of $\bar{M}_{w,app}$ against concentration, together with a line calculated from the fitted parameters, made to show the dependence.

1. Van Holde, K. E. & Baldwin, R. L. (1958). Rapid attainment of sedimentation equilibrium. *J. Phys. Chem.* **62**, 734-43.
2. Casassa, E. F. & Eisenberg, H. (1964). Thermodynamic analysis of multicomponent solutions. *Adv. Prot. Chem.* **19**, 287-395.
3. Hayes, D. B., Laue, T. & Philo, J. (1995). Sednterp. RASMB.
4. Johnson, M. L. & Straume, M. (1994). Comments on the analysis of sedimentation equilibrium experiments. In *Modern Analytical Ultracentrifugation* (Schuster, T. M. & Laue, T. M., eds.), pp. 37-65. Birkhäuser, Boston, USA.